doi:10.1017/S143192762200232X
Microsc. Microanal. 28 (Suppl 1), 2022

Examining the Relationship Between Local Polarization and Modulation Variations in a Relaxor Ferroelectric Tetragonal Tungsten Bronze By 4D STEM

Stephen D. Funni[1], Elizabeth C. Dickey[1]

[1.] Department of Materials Science and Engineering, Carnegie Mellon University, Pittsburgh, PA, USA

Relaxors and ferroelectrics are important functional material types especially in transducer and capacitor applications. In the search for lead-free alternatives for these applications tetragonal tungsten bronze (TTB) oxides have been examined due to their flexible chemistry and wide range of properties.[1] TTB oxides are capable of hosting a wide range of compositions and generally have either relaxor or classical ferroelectric behavior [2]. TTBs often possess commensurate or incommensurate (IC) structural modulations, and the modulation type has been empirically related to the type of ferroelectricity [2]. The modulation arises from tilting within the oxygen-octahedral network, but also produces displacements on A2 sites.[3] Various tilt patterns have been proposed for IC structures, but due to experimental challenges (e.g. limited TEM resolution, [4] the weakness of satellite peaks in x-ray diffraction [5]) they have not been conclusively demonstrated. An Ama2 space group unit cell was proposed as a commensurate approximation of the IC modulation for TTBs [6] and is shown in Figure 1. In previous work, we showed from high-angle annular dark field (HAADF) scanning transmission electron microscope (STEM) imaging that the IC modulation of the A2 sites in the relaxor $Ba_5Sm_1Sn_3Nb_7O_{30}$ (BSSN) is discontinuous and its correlation length highly anisotropic [7]. Furthermore, we observed that some regions in the images lacked modulation-related displacements visible in the projection. We concluded this was due to the presence of two orientational variants of the modulation, one in the plane of the image and one out-of-plane, each of which break the ideal tetragonal symmetry. This conclusion was supported by diffraction and conventional dark field imaging. It also agrees with the proposed Ama2 approximation, in that the two orientations may each be present in different mesoscopic regions within a grain while yielding a tetragonal structure globally. Additionally, we observed short-range clusters of polar displacements on the B1 site which tended to be found near boundaries between the modulation variant regions. Due to the small field of view in the atomic-resolution images, this correlation was not statistically robust. Furthermore, because HAADF imaging is far more sensitive to heavy elements, we were unable to image the oxygen sublattice, leaving open the question of octahedral tilting.

To build upon our previous work, we present analysis of BSSN using 4-dimensional STEM (4D STEM) data. 4D STEM is a technique in which a 2D diffraction pattern is collected corresponding to each real-space pixel in the 2D probe scan pattern. This allows many different types of images to be produced from a single dataset by applying virtual detectors to the diffraction patterns [8]. Additionally, light and heavy elements can be simultaneously observed by integrated center-of-mass imaging (iCOM), a more quantitative and, potentially higher resolution, technique than conventional differential phase contrast with a quadrant detector.[9] We apply 4D STEM to characterize the IC structure of BSSN through two types of experiments: nano-beam electron diffraction (NBED) and atomic resolution iCOM imaging.

In the NBED experiment, a small convergence angle of 1.1 mrad is used to prevent overlap of the Bragg disks and yield a probe size of approximately 1 nm, close to the **c** lattice parameter of the Ama2 unit cell. A large probe step size can be used in NBED experiments and this allows collecting data over a large field of view, on the order of 1 μm^2 [8]. Figure 2a & b show simulated position-averaged

converged-beam electron diffraction (PACBED) patterns obtained from the Ama2 unit cell along the [100] and [010] zone axes, corresponding to modulation orientations in and out of the zero-order Laue zone plane, respectively. (All simulations were preformed using the abTEM package in Python [10].) Note the rows of superlattice disks in the [100] pattern, indicated by the arrows. In the [010] pattern, however, satellite disks are absent except at higher scattering angles (also indicated by arrows) where Ewald's sphere intersects the reciprocal lattice points corresponding to the out-of-plane modulation. Applying virtual detectors to measure the intensity of the two types of satellite disks in the experimental data, we map modulation orientation over a large field of view. In a similar manner, the local polarization of the sample is measured in the same dataset by calculating the normalized intensity difference between the 002 and $00\bar{2}$ conjugate disk pair [11]. This pair is chosen over the $001/00\bar{1}$ due to its greater absolute intensity and sensitivity to polar displacements in simulated patterns. By comparing the map of the modulation orientation with that of the polarization, we reveal the relationship between the IC modulated structure and local material properties in BSSN.

To identify the modulation-related displacements in both the oxygen octahedra and cation sublattices, we image the atomic structure using iCOM. The data is collected using a convergence semi-angle of 30 mrad and a 300 keV beam energy to achieve a sub-angstrom probe size. Figure 2c shows a simulated iCOM image of the Ama2 structure along the [100] zone axis using these imaging parameters. A gaussian blur was added to the image to account for the effect of finite source size. The set of projected oxygen positions resolved by this technique indicate the projected tilt amplitude of the B2-site oxygen octahedra. By simultaneously imaging the cations and a portion of the oxygen sublattice, we measure the oxygen octahedral tilting pattern present in BSSN, relate it directly to our previous observation of cation displacement ordering, and evaluate the proposed Ama2 structure.

Using 4D STEM techniques we quantitively study the IC modulation in BSSN, showing how the modulation orientation and related structural displacements influence polarization at the nanoscale.

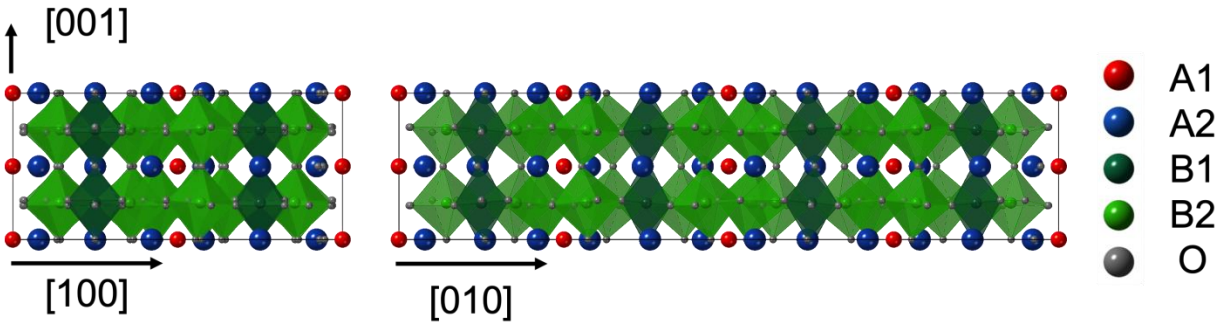

Figure 1. [010] and [100] zone axis projections of the proposed Ama2 commensurate approximation of the IC modulation in BSSN.

https://doi.org/10.1017/S143192762200232X Published online by Cambridge University Press

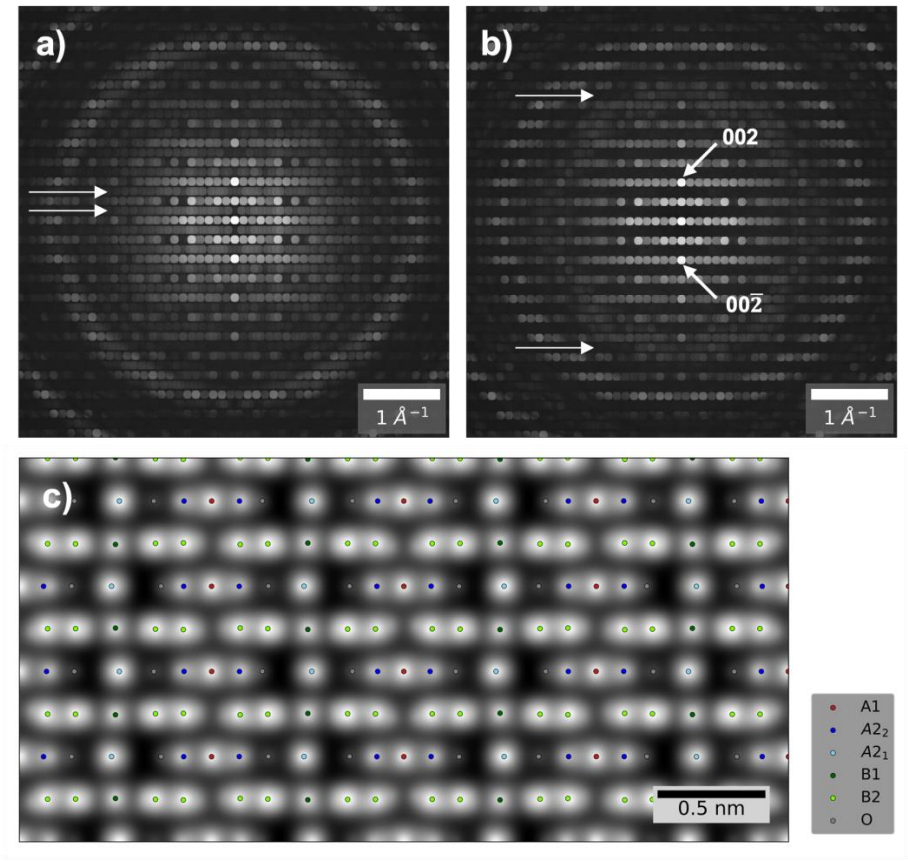

Figure 2. PACBED patterns simulated from the Ama2 unit cell of BSSN for the a) [100] zone axis with modulation vector in-plane and b) [010] zone axis with out of plane modulation vector. Arrows in a) and b) indicate rows of superlattice disks corresponding to the modulation and, in b) the 002 / 00$\bar{2}$ conjugate disks are also noted. c) [100] zone axis iCOM image calculated from a simulated 4D STEM dataset using the Ama2 commensurate structure. Note the resolved oxygen positions which reveal the octahedral tilting pattern.

References:

[1] V. V. Shvartsman, D. C. Lupascu, J. Am. Ceram. Soc. **95** (2012), p. 1.
[2] X. Zhu et al., Chem. Mater. **27** (2015), p. 3250.
[3] I. Levin et al., Sci. Rep. **7** (2017), DOI 10.1038/s41598-017-15937-x.
[4] L. A. Bursill, J. L. Peng, Acta Cryst **43** (1987), p. 49.
[5] T. Woike et al., Acta Crystallogr. Sect. B **59** (2003), p. 28.
[6] I. Levin et al., Appl. Phys. Lett. **89** (2006), DOI 10.1063/1.2355434.
[7] S. D. Funni et al., APL Mater. **9** (2021), 091110.
[8] C. Ophus, Microsc. Microanal. **25** (2019), p. 563.
[9] I. Lazić, E. G. T. Bosch, S. Lazar, Ultramicroscopy **160** (2016), p. 265.
[10] J. Madsen, T. Susi, Open Res. Eur. **1** (2021), p. 24.
[11] K. Tsuda, A. Yasuhara, M. Tanaka, Appl. Phys. Lett. **103** (2013), DOI 10.1063/1.4819221.

https://doi.org/10.1017/S143192762200232X Published online by Cambridge University Press